This article has been accepted for inclusion in a future issue of this journal. Content is final as presented, with the exception of pagination.

System Design and Realization of a Solar-Powered Electric Vehicle Charging Station

Samir M. Shariff, *Senior Member, IEEE*, Mohammad Saad Alam, *Senior Member, IEEE*, Furkan Ahmad, *Student Member, IEEE*, Yasser Rafat, M. Syed Jamil Asghar, *Senior Member, IEEE*, and Saadullah Khan

***Abstract*—The alarming situation of global warming leads to the full adoption of the renewable energy-based transportation system. However, their sustainable deployment at a mass level has been a challenging task. This article presents the design aspects and practical implementation of the modern solar-assisted level-2 electric vehicle charging station which is controlled by a Type-1 vehicle connector. The designed model is developed in MATLAB/Simulink environment, the circuit operation is examined and its methodological model is derived to study the parametric design features. Furthermore, the complete hardware setup has developed to test the performance of the power factor correction under the steady-state condition with respect to variation in load for the input of 3 kW, 230 Vrms at 1-phase, 50 Hz rated, and to produce a 48 V buck converter dc output. The 6.4 kW solar photovoltaic (PV) charging station, installed at the Centre of Advanced Research in Electrified Transportation building parking area in Aligarh Muslim University campus, selected as a case site. Moreover, the controller circuit is simulated in PROTEUS software and a prototype model has been tested in the lab. The study is performed on a 10 kWh lithium-ion battery pack on a bright sunny day at standard test condition of the solar panel.**

***Index Terms*—Converter topology, electric vehicle (EV), EV charging infrastructure, solar photovoltaic (PV).**

I. Introduction

THE deterioration of air quality, issues of global warming, and continuous depletion of fossil fuels are serious issues to consider. The conventional electricity generation sector and the transportation sector are the major contributors to these issues. The advent of the renewable energy-based generation and electrification of transportation fleet is aimed to provide a sustainable solution to these issues. The need for a green and sustainable mode of transportation and the advancement of a battery technology has sparked interest in electric vehicles (EVs) as a viable mode of transportation.

Due to the intermittent nature of the renewable energy particularly solar photovoltaic (PV), storage technologies such as batteries need to be deployed to smooth out the fluctuating power output. The battery pack of the EVs can be leveraged for this purpose making EVs more feasible than internal combustion engine (ICE) vehicles. In this article, a 3 kW PV-EV charger as recharging as well as discharging of the vehicle for 3 kW rated power output. A pulsewidth modulation (PWM)-based charging control strategy has been tested in the lab. As EVs or PHEVs are equipped with high voltage batteries to increase the driving range and improve the fuel efficiency, a universal input charging station for EVs is developed to deploy it commercially for the quicker appropriation of the electrified transportation framework in the country.

Thus, in the last decade, numerous researchers have contributed toward the technological advancements and fruitful implementation of the solar-powered EV charging station. In [2], a concept of grid-integrated solar PV-battery recharging framework to enhance the system reliability is proposed. In [3], an energy management system (EMS) for xEV-based charging infrastructure integrated with an energy storage system (ESS) in a smart microgrid environment is covered. Khan *et al.* [3] have reviewed the various technique related to the solar-powered EV charging station. Shafaati Shemami *et al.* [4] and Luo *et al.* [5] present a vehicle-to-home strategy for utilizing distributed generation such as the solar power to deal with the complexity of dynamic electricity prices.

Some other papers have also published in the literature in the context of EV-PV charging schemes. Thus, Sahoo *et al.* [6] have studied the modeling of a solar PV-based EV charging that is suitable for dc quick charging arrangement in order to minimize the grid stress through a vehicle-to-grid scheme. Ahmad *et al.* [7] have presented an optimal EMS for a coordinated charging scheme and the proposed methodology has been practically realized by setting up a hardware model of a PV-based charging system. However, Cao *et al.* [8] have examined the plug-in EVs integrated renewable energy source for desirable cost and emission reductions. Furthermore, Muttaqi *et al.* [12] have proposed an algorithm for optimal scheduling of home-based EV charging. The proposed model also

Manuscript received January 12, 2019; revised May 9, 2019 and July 7, 2019; accepted July 25, 2019. This work was supported in part by the Centre of Advanced Research in Electrified Transportation, Aligarh Muslim University, Aligarh, under FAME India Mission, and in part by the Department of Heavy Industry, Government of India. *(Corresponding author: Furkan Ahmad.)*

S. M. Shariff is with the Department of Electrical Engineering, Faculty of Engineering, Taibah University, Medina 42353, Saudi Arabia (e-mail: samshariff@yahoo.com).

M. S. Alam is with the Department of Electrical Engineering and the Centre of Advanced Research in Electrified Transportation, Aligarh Muslim University, Aligarh 202002, India (e-mail: saad.alam@zhcet.ac.in).

F. Ahmad, M. S. J. Asghar, and S. Khan are with the Department of Electrical Engineering, Aligarh Muslim University, Aligarh 202002, India (e-mail: furkanahmad@zhcet.ac.in; mjamil.ee@amu.ac.in; saadullahkhan@zhcet.ac.in).

Y. Rafat is with the Department of Mechanical Engineering, Aligarh Muslim University, Aligarh 202002, India (e-mail: Yasser.rafat@zhcet.ac.in).

Digital Object Identifier 10.1109/JSYST.2019.2931880

This article has been accepted for inclusion in a future issue of this journal. Content is final as presented, with the exception of pagination.

consist the forecasted renewable energy generation and home demand.

Furthermore, Konjedic *et al.* [9]–[11] have focused on the optimal designing of the power electronic converter for the solar-based charging station. The state-of-the-art technological innovation in the field of the power electronics for the application of the electrified transportation has been discussed in [13].

Mouli *et al.* [14] have presented a solar-powered battery charging scheme under partial shading of solar panels. The proposed system uses the Cauchy–Gaussian sine cosine optimization method for the maximum power point tracking. In [15], a direct solar-powered dc-EV recharging system has developed which increases the overall efficiency by reducing the ac/dc conversion stage.

A large portion of [2]–[15] has devoted to introducing scientific/logical approaches to deal with various design and implementation issues. Besides, these works talk about hypothetical instead of functional contextual investigations, utilizing restricted and accepted information, as opposed to genuine and complete informational collections on account of this article. Again, while studying deeply the literature cited from [7] to [13], the conclusion is that besides several novel techniques and methods, the practical approach of a charging process control strategy has not fully been incorporated and implemented.

All these require study, design, and integration of an off-board EV charger with solar photovoltaic as a charging source, realizing the need for sustainable deployment of EVs and PHEVs, which is the focal point of this article. Subsequently, the key contribution of this article is as follows.

1) This article presents practical design considerations for a universal input EV battery charger to be used in a plug-in hybrid vehicle. Stringent operating conditions were imposed on the charger for applications in a solar-powered plug-in EV.
2) The EV battery charger circuit should be capable of maintaining a high power factor at the front end and the low ripple current at the output. For this purpose, a PWM boost rectifier cascaded with a bidirectional dc–dc converter has been proposed in this article. Operation of the circuit has been analyzed and a mathematical model for the charging operation in continuous conduction mode (CCM) is formulated.
3) For the control of the vehicle charging circuit, a commonly used PWM-based controller through Type-1 connector is implemented.

The rest of this article is organized by elaborating the text in nine different segments as follows. Section II discusses the design of the solar photovoltaic (SPV)-EV charging station installed at the Centre of Advanced Research in Electrified Transportation (CARET), Aligarh Muslim University (AMU) campus and is taken as the case site for the study. Section III presents a comprehensive overview of the methodology adopted in this article. Section IV deals with the EV supply equipment (EVSE), its architecture, control process simulation, and testing of a prototype model based on the combined charging system (CCS) protocol. Section V describes the design of the SPV-based EV charging station. It comprises the PV generator design, EV charging load design, ESS and converter design, etc. Section VI describes the modeling of the EV charger (bidirectional) converter topology with complete design and working of the circuit. Simulations of the converter and communication circuits are discussed in Section VII. Section VIII represents the hardware setup with experimental results. Finally, Section IX draws the main conclusions and contributions of this article with summarized challenges and future work.

TABLE I
DAILY AVERAGE HOURS/MONTH OF SUNSHINE BY LATITUDE ALTITUDE (NREL DATA)

Location	Country	Sea Level	Latitude	Longitude
Aligarh	*India*	*227 m*	*77 E*	*28 N*
Month	**sunshine hours**		Month	**sunshine hours**
January	6.9		**July**	5.3
February	7.7		**August**	5.7
March	7.7		**September**	7.3
April	8.7		**October**	8.7
May	8.5		**November**	8.2
June	6.5		**December**	7.0

II. Solar Photovoltaic Charging Station (SPVCS) Installed at CARET, AMU

According to meteorological data of selected site taken from the NREL, Aligarh, is situated 78 N, 27 E. The estimated values of "peak sun hours" (a numerical equivalent value for the aggregated time in which averages solar intensity is 1 kWh/m^2) are listed in Table I. It is concluded that the average sunshine hours is 7.4.

The system comprises of "6.4 kW solar PV-EV charging parking lot" working as a microgrid, consists of 20 solar panels of Vikram Solar company (each panel rating is 320 W_p, 37 V, 8 A), covering an area of $56 \times 16 = 896$ ft^2. It can supply a charging load of 5–6 kW per day (8 h). The plant is installed in CARET building parking area (see Fig. 1), AMU campus. The PV module electrical characteristics are calculated at standard test conditions, where the ambient temperature is 25 °C, irradiance (radiant flux) is 1000 W/m^2, and sun's spectrum should be at AM 1.5. Installation and replacement cost, and operating and maintenance (O&M) cost per kW of solar PV are taken as INR 60 000, INR 30 000, and INR 2000/year, respectively.

III. Proposed Framework for SPVCS of EVs

Fig. 2 outlines the block schematics of the proposed charging system installed in the university parking area. The charging station is supplied from two sources used for recharging the vehicles parked under a shed, viz., the conventional utility grid electricity and also solar PV-based electricity. Hence, the charging station supplies the solar power to the vehicles coming for charging by utilizing solar energy during the day time and the conventional grid power in the night hours [16]. The PV system modeling depends on the components of the block that comprises the connection under a PV framework, i.e., PV generator, charge controller, battery storage, solar hybrid inverter, EV charger, and EV battery as a load. Every component will be analyzed and presented separately and as a whole in this article.

This article has been accepted for inclusion in a future issue of this journal. Content is final as presented, with the exception of pagination.

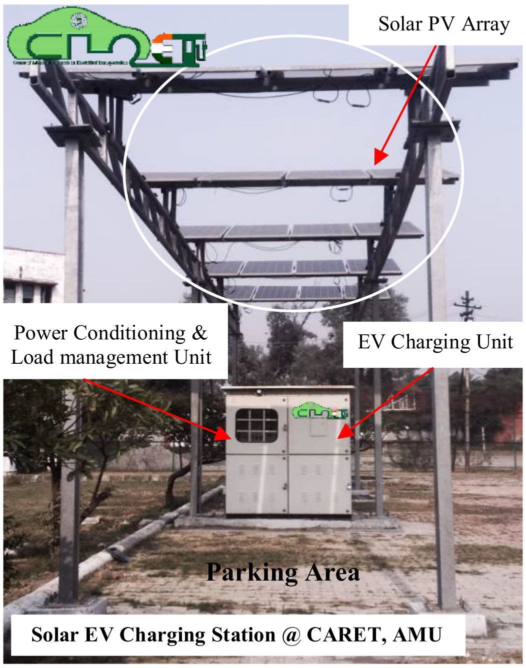

Fig. 1. Solar PV charging station at CARET, AMU, Aligarh.

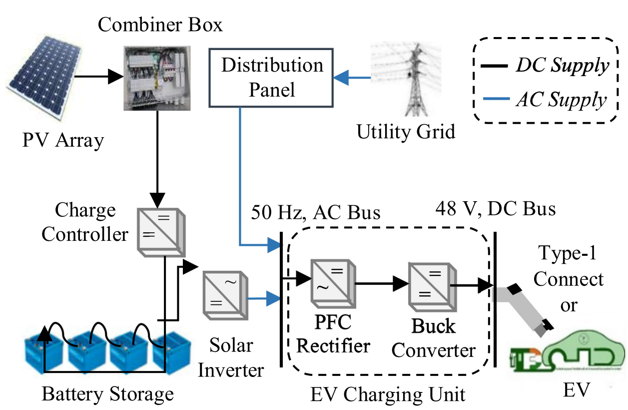

Fig. 2. Diagram showing the block elements of the SPVCS.

Fig. 2 shows the PV array, components of the solar conversion system and EV charging system, and the power flow. The black arrows represent the flow of the dc power produced by the PV panels, whereas the blue arrows represent the flow of the ac power drawn from the electric utility grid and the solar inverter. The fluctuations and intermittency in a solar generation can be removed by the dc–dc charge controller and battery storage, respectively. As the station is a standalone solar hybrid system (no grid reference is needed for the operation of the system), hence, the increased load demand can be met by the ac grid, but the surplus generation could not be sent back to the grid.

The NEC-2017 Article-625 defines the EVSE as "The conductors, including the grounded, ungrounded, equipment grounding, etc., the EV attachment plugs, connectors, and all other devices, fittings, apparatus or power outlets specifically installed for delivering the electrical energy from the wiring of the premises to the EV." Essentially, the charging operation is performed by the charger (onboard/off-board) [18] and other equipment outside the vehicle chassis to deliver the electrical energy required for recharging the lithium-ion (LI) battery pack. Primarily the EVSE, specifically those for the use under the CCS level 1 or level 2, is an equipment (for safety and protection of the onboard charger), not a complete charger that connects directly with the car battery pack, but the function is rather to provide an interface for a power supply system to the charger (onboard/off-board type) (see Fig. 3) [19].

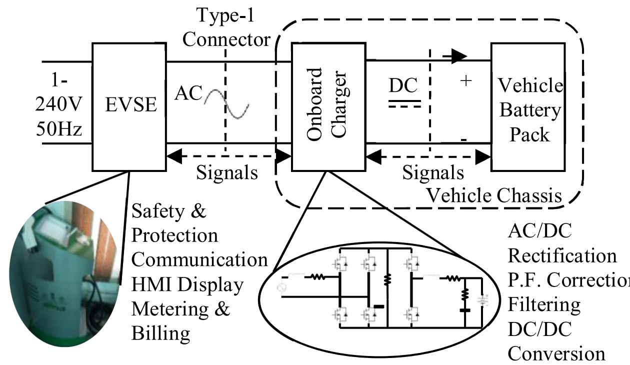

Fig. 3. Vehicle charging system.

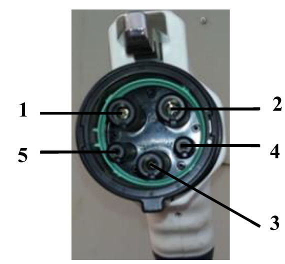

Fig. 4. Type-1 conductive coupler.

Type-1 is a smart connector, which offers required protection and control functions approved by International Electrotechnical Commission (IEC) and Society of Automotive Engineers (SAE) standards where the vehicle is connected to the utility grid/solar PV. Fig. 4 shows the control circuitry used for the EV charging system. A number of other voluntary features for facilitating the procedure to be followed for guaranteeing the specific purpose by authorized users.

A. *Signaling System Under the CCS Charging Standard*

The CCS is based on open and universal standards for the EVs. The CCS combines single-phase with rapid three-phase charging using alternating current at a maximum of 43 kW, as well as direct current charging at a maximum of 200 kW and the future perspective of up to 350 kW—all in a single system. Essentially, the standard outlines in what way an EV charging infrastructure communicates with, connect with, and control the charging of the car. Hence, the EVSE provides the linkage between the vehicle and the grid (household power) or solar PV. It serves as a smart connector that "handshake" the vehicle and communicates to enable safe charging.

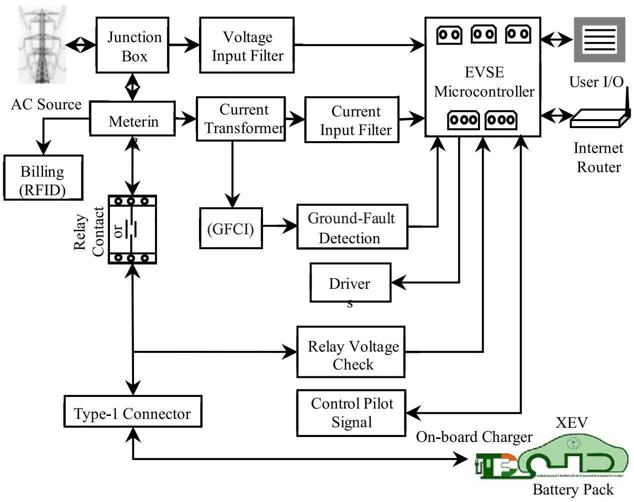

Fig. 5. Vehicle charging control architecture block schematic.

Now the Type-1 applies under the CCS protocol and has been adopted worldwide by all the passenger vehicles manufacturers globally [21]. Different pin configurations are ac line 1 (Phase), ac line 2 (Neutral), ground, control pilot, and proximity detection signals, as shown in Fig. 4.

Proximity-Earth (PE): To prevent the car movement as it is connected with the EVSE.

Control-Pilot (CP): A $\pm$ 12 V 1 kHz square wave pulse signal is generated on the Pilot-Pin by the EVSE to sense and communicate the vehicle to control the charging process and check the maximum permissible current limit.

Fig. 5 shows the charging controller circuit schematics. Various functions are performed through the EVSE by using the relays of high power rating in the circuit. For safely operating the relay, a driver with a suitable protection circuit should be applied [20] as the following.

1) An overcurrent relay (solid state type) for short circuit and overload protection.
2) An electronic contactor switch for latching-up the connector with the supply.
3) A controller circuitry which interfaces the onboard charger and provides line-to-ground fault protection (see ground-fault circuit interrupter (GFCI) in Fig. 5).
4) Displays and indicators on the peripheral to show the alarm status and help the users to understand the working sequence.
5) Connecting cable from the EVSE to the onboard receptacle in the vehicle chassis.
6) A female connector (conductive type) to plug into the male counterpart on the vehicle.

B. *Operating Sequence of the PWM-Based Vehicle Charging Controller*

The charging sequence and its related system activities are specified by the CCS protocol. Light emitting diode (LED) indicators viewed easily from a distant location could make the owner to determine the EVSE status. Hence, through these colored indicators, the following mentioned states of charging can convey easily (see Table II):

1) the charging station is active, i.e., ac supply is available;
2) the connector is connected to the vehicle, i.e., not charging but connected mechanically;
3) charging starts, i.e., in progress through electrical connection;
4) fault or alarm condition.

TABLE II
PWM-Based Charging Control Strategy Based on the CCS Standard [21]

Total Resistance between CP-PE	Open circuit	2700 ohm (Ω)	880 ohm (Ω)	240 ohm (Ω)		
Resistors R2 + R3 = 2740 Ω	-	- 2740 Ω	1300 Ω 2740 Ω	270 Ω 2740 Ω		
Voltage Measured: CP-PE	+12 V	+9 V ±1 V	+6 V ±1 V	+3 V ±1 V	0 V	-12 V
State of charging	State A	State B	State C	State D	State E	State F
Charging status	standby	Vehicle detected	Ready (charging)	With ventilation	No power	Error

IV. Description of the Component Used in the Proposed Architecture for the SPVCS

Herein, the design and description of different solar PV system components for the EV charging application at the parking lot is presented. The proposed charging station is a photovoltaic grid connected power system operating in a hybrid mode. It is basically an interconnected system of components that converts directly solar irradiance into electricity and usually comprises of the PV panels, utility grid, battery storage, converter system (inverter, charge controller, etc.), EV charger (PFC rectifier, buck converter, etc.), and the system load (EV battery in this case) which are described one by one in the following sections.

A. *Solar PV as Generating Source*

The PV panel dimensions, solar radiation falling on the panel, and PV module temperature rise are the issues by which the solar power output varies [22]. The power output can be calculated as

$$P_{\mathrm{pv}}(t) = \mathrm{CI}(t)\, I_{\mathrm{SC}} \left(1 + \frac{33}{1000}\cos\left(\frac{360d}{365}\right)\right) \times (\sin\varphi\sin\delta + \cos\varphi\cos\delta\cos(\omega t)) \tag{1}$$

$$\omega = \text{minutes before noon}/4 \tag{2}$$

$$\delta = 23.45\,\mathrm{Sin}\,\{360\,(d + 284)/365\} \tag{3}$$

where $P_{\mathrm{pv}}(t)$ is the PV generated power as a function of time (t), I_{SC} is termed as a solar constant, and $\mathrm{CI}(t)$ is the clearing index at t. Now, hour angle ω can be calculated by (2) (approximated as $\pm 15°$/h, $+$ for morning and $-$ for the afternoon), while the decline angle of the sun δ by (3) (d signifies the day). The geographical latitude is φ and 27° is taken (user dependent). For the PV generation, consider an array of 20 panels (2 series modules $\times$ 10 parallel strings) where each panel is rated at

This article has been accepted for inclusion in a future issue of this journal. Content is final as presented, with the exception of pagination.

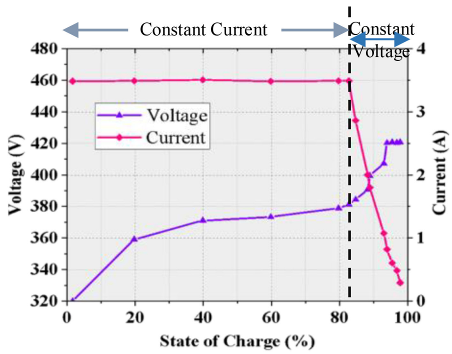

Fig. 6. Charging profile based on the SOC of the LI battery pack [24].

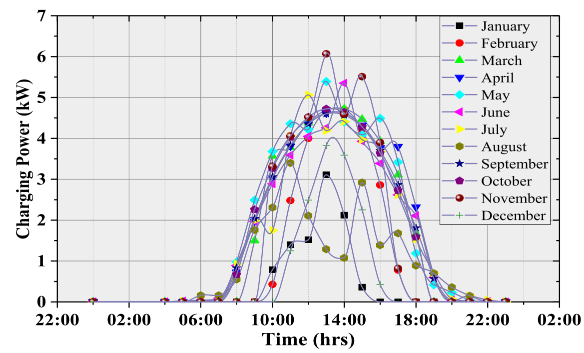

Fig. 7. Frequency of the charging station usage.

300 W_P. The performance and characteristics of this array are evaluated for a module temperature at 25 °C and specified values of solar irradiance, i.e., 100–1000 W/m^2 [23].

Monthly average global horizontal irradiance data (from the NREL database) show that the SPV generation is more in May following April to June, whereas July to September leads to lower power generation due to rain, and the lowest one recorded during winter/foggy season (December to January).

B. ESS as EV Charging Load

There are few currently available EVs in India. These battery electric vehicles (BEVs) have 4–6 seat capacity with an approx.120 km driving range. The LI battery pack, used as ESS, has a typical 11–13 kWh of capacity. The maximum speed is 120 km/h achieved by consuming 0.1 kWh/km energy.

The energy supplied to the vehicle is defined by the difference in the initial and final states-of-charge (SOC) of the battery pack. The mathematical expression for calculating E_{req} (energy required) for a specific type of BEV is

$$EE_{\text{req}} = \Delta\text{SOC} \cdot C_{\text{bat\_BEV}} \tag{4}$$

where E denotes the total of the energy and $C_{\text{bat\_Bus}} =$ Battery C rating for selected BEV ($\Delta\text{SOC} = 20\%$ to 100% in this case).

In light of the charging characteristics of a particular cell, the LI battery pack charging profile can be plotted as shown in Fig. 6.

1) Vehicle Parking Scenario: The study of vehicle parking statistics reveals how much time does one vehicle take for charging and how many vehicles could be charged at a time per day. Basically, it deals with the available solar generation, types of charging (i.e., the voltage and power rating of the charger) and the battery chemistry used in the EVs. It characterizes the four specialized guidelines of the charging stations that are presently used, i.e., Level-1, Level-2, Level-3, and dc fast charging.

In India at the administrative level, especially in medium-scale organizations, a worker usually works for up to 11 h per day and six days per week. The vast majority of the Indian organizations and MNCs and government places will, in general, pursue five days, 8–9 h each day operating schedule. These perceptions demonstrate that vehicles are ordinarily parked for an adequate amount of time in a day to such an extent that it is conceivable to utilize solar generation specifically for the PEV charging at the parking lot without utilizing expansive ESS. The frequency of the charging station usage is represented in Fig. 7. Hence, the idea of workplace daytime charging by utilizing the PV panels is examined in Fig. 7.

C. Battery Storage and Converter Design

Another significant component of the solar PV off-grid system is the battery storage. The storage is needed in such systems, owing to the variations in the PV generated output. When sunlight is available, the photovoltaic system supplies the load directly and the surplus power is stored to the battery storage. While during night hours, or when sunlight is not available, the consumer load demand can be fulfilled by the battery storage. For a solar charging model, a separate battery bank (Lead Acid) as ESS is used. The nominal rating is 12 V $\times$ 4 = 48 V, and of 150 Ah (7.2 kWh). The rate of charging and discharging of a battery is a key parameter which decides its life and performance and also affects the power output factor related to any battery bank, as given in (5). The formula for the SOC calculation is given as

$$\text{SOC }(t) = (1 - Q)\,\text{SOC }(t-1) + \frac{P_{cd}\Delta(t)\,e_{cd}}{E} \tag{5}$$

where the SOCs, SOC (t) and SOC($t-1$), are calculated at a time interval of (t) and ($t-1$), respectively, Q is the discharge rate per hour,p_{cd} is the power of charging and discharging, e_{cd} is the efficiency of charging and discharging, and E denotes the total of the energy stored in the battery. The battery SOC is the key parameter which governs the charging time and energy required by the vehicles parked for charging under the garage.

The converter system in the standalone solar PV necessitates a control strategy to be applied to all the supply systems that define the relations between different elements. The battery usage as an energy storage component necessitates the integration of the charge regulator (controller). The function of this device is to manage the flow of energy in the PV source, battery storage, and EV charging load by taking the data regarding the battery terminal voltage with the constraints of its minimum and maximum allowable limits.

The converter system is for power conversion from ac-dc or vice-versa. The installation cost and replacement cost are, for

This article has been accepted for inclusion in a future issue of this journal. Content is final as presented, with the exception of pagination.

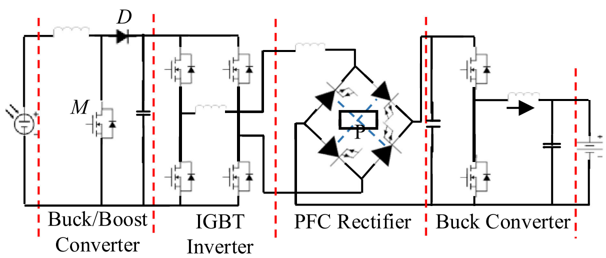

Fig. 8. Solar PV-EV charging circuit topology [25].

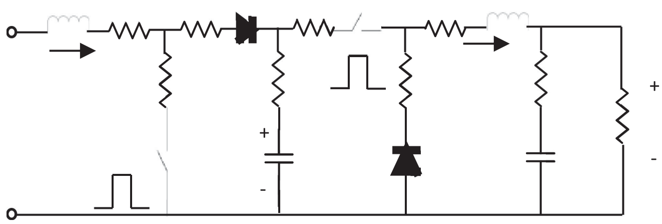

Fig. 9. EV battery charger equivalent circuit.

1 kW of the converter, considered as INR 35 715 and INR 10 000, respectively. A total of a 7 kW converter capacity is designed for the simulation as the PV installed capacity is 6.4 kW, 15 years inverter lifetime, and 91% efficiency are taken for this case. A rectifier capacity is considered to be 100% relative to the inverter of 85% efficiency. A 1 kW converter O&M costs is INR 5000 per year.

V. Modeling of the EV Charger Converter Topology

The circuit topology made out of a bidirectional PWM boost rectifier (ac/dc) operates in cascade connection by means of a bidirectional dc/dc converter to be proposed for the application as the EV battery charging circuit, as shown in Fig. 8.

In this working condition, the PFC operation could be realized through a PWM rectifier by operating it in a boost mode, whereas the buck operation could be realized through the dc/dc converter. In addition, hence, in a reverse mode of the operation, the dc/dc converter function is in a boost mode while the rectifier operates in an inverter mode. As the circuit runs mostly in the charging mode to charge a PHEV, the considerations of the circuit parameter will depend on the PWM rectifier in the boost operation and the dc/dc converter in the buck condition. Subsequently, the practical design considerations for ratings of the components are determined for the charging mode as it were.

Here, switchesS_1, S_2, S_3, and S_4 combines to the ac/dc boost rectifier (Q_{boost}), while S_5 and S_6 to the dc–dc buck converter (Q_{buck}). Therefore, depending on the operating conditions, the charging circuit can operate in four different modes, i.e., when both Q_{boost} and Q_{buck} are ON and OFF, and when Q_{boost} ON but Q_{buck} OFF or vice-versa, etc. The mathematical model (see Fig. 9) of the components for the circuit operation when both are ON is as follows.

The input inductor current differential equation is

$$L_1 \frac{di_{L1}}{dt} + (r_{L1} + r_{S1})\, i_{L1} = V_S \tag{6}$$

$$\frac{di_{L1}}{dt} = \frac{V_S}{L_1} - \frac{(r_{L1} + r_{S1})}{L_1} i_{L1}. \tag{7}$$

The output inductor current differential equation is

$$(R_{C1} + R_{L2})\, I_{L2} + L_2 \frac{dI_{L2}}{dt} + R_{\text{out}} I_{\text{out}} = V_{C1} \tag{8}$$

$$L_2 \frac{dI_{L2}}{dt} + (R_{C1} + R_{L2})\, I_{L2}\; I_{C2} R_{C2} + V_{C2} = V_{C1}. \tag{9}$$

The output voltage equations can be expressed as

$$V_{\text{out}} = R_{\text{out}} I_{\text{out}} = \frac{R_{\text{out}} R_{C2}}{(R_{C2} + R_{\text{out}})} I_{L2} + \frac{R_{\text{out}}}{(R_{C2} + R_{\text{out}})} V_{C2}. \tag{10}$$

The dc bus capacitor voltage differential equation is

$$C_1 \frac{dV_{C1}}{dt} = -\, i_{L2} \quad \frac{dV_{C1}}{dt} = -\frac{1}{C_1}\, i_{L2}. \tag{11}$$

The output capacitor voltage differential equation is

$$i_{C2} = C_2 \frac{dV_{C2}}{dt} \tag{12}$$

$$V_{C2} + i_{C2}\,(r_{C2} + R_{\text{out}}) = I_{L2} R_{\text{out}}$$

$$i_{C2} = -\frac{V_{C2}}{r_{C2} + R_{\text{out}}} + \frac{R_{\text{out}}}{r_{C2} + R_{\text{out}}} I_{L2}. \tag{13}$$

Combining (12) and (13) results in

$$\frac{dV_{C2}}{dt} = -\frac{1}{C_2 (r_{C2} + R_{\text{out}})} V_{C2} + \frac{R_{\text{out}}}{C_2 (r_{C2} + R_{\text{out}})} I_{L2}. \tag{14}$$

The boost mode working of the PWM rectifier depends on gate pulse triggering of the individual switch combinations subjective to every switching sequence to trace the current through an inductor by a sinusoidal curve defined by the digital signal processor (DSP)-based microcontroller. Due to the high-frequency switching pulses than that of line frequency (50 Hz), in one complete cycle, the PWM rectifier input voltage can be observed as consistent. The operation of the circuit can be realized in both, i.e., CCM and discontinuous conduction mode (DCM). Now in the DCM mode, the current through an inductor reaches zero at the end of every switching cycle. Contingent upon the rating of the boost inductor with a specified duty ratio, the PWM rectifier could have the self PFC control which means the line voltage should be in the same phase as the line input current with no regulation on the supply (input) side. Be that as it may, in the DCM mode, due to the intermittency in the current input, the capacitor rating at the dc bus should be sufficiently higher to maintain the balance of the power (at a particular instant) between the output and input. In the CCM mode, the higher rating of the capacitor at dc bus is additionally expected for reducing the ripple in dc bus voltage and, hence, eliminating the low-pass filter circuit from the output side.

The operation will likewise be examined in the accompanying segments. As the given EV charging circuit is applicable for moderately high power circuit, the CCM operating mode will be explained.

A. Circuit Components Rating Considerations

The equivalent circuit is shown above (see Fig. 9) reveals that the circuit proposed can be denoted by the cascade operation by connecting the dc/ac PWM boost converter to the dc/dc buck converter for the EV battery charging mode. Now, the circuit parameters and its performance can be studied by examining the commonly derived relations applicable to these circuits.

1) Inductor Design: There are two types of inductors used in the circuit, dc (Buck) inductor and ac (Boost) inductor. The ripple in the charging current of the battery is of much importance with the maximum allowable ripples is typically listed in the manufacturers' data sheet, whereas for the PFC criteria, the current input has to be modified so that it is in the same phase as the voltage. Now, as the battery terminal voltage output at the buck converter should be constant, hence, the dc inductor current (peak to peak value) ripple is characterized as

$$\Delta I_{\mathrm{DC}} = \frac{V_{\mathrm{BUS}}\langle d_{\mathrm{DC}}\rangle\left(1-\langle d_{\mathrm{DC}}\rangle\right)}{f_s L_{\mathrm{DC}}} = \frac{V_B - \frac{V_B^2}{V_{\mathrm{BUS}}}}{f_s L_{\mathrm{DC}}} \qquad (15)$$

where f_s is the switching frequency.

The ripple content in the ac current of the inductor in the CCM operating mode is characterized as

$$\Delta I_S = \frac{V_S\langle d_{\mathrm{AC}}\rangle}{f_s L_1}. \qquad (16)$$

For the higher ratings of L_1, the ripple content in the inductor current reduces and the current input pursues the reference better. Hence, the total harmonic distortion (THD) value also reduces (<5%). In this way, the rating of L_1 must be characterized for the maximum input voltage rating in which the ripples in the current will also be maximum. Higher f_s value additionally added the inductor core loss leading to the rise in the temperature.

The higher current capacity needs thick winding wire wounded on a sufficiently big core to avoid the saturation of the core. Currently, a higher rating of the inductance implies a number of turns and, consequently, enough space for winding resulting in a huge increment in the weight and size. Then again, the size could be decreased by applying higher f_s (switching frequency), given that the size of the core is sufficiently large enough for accommodating more turns. As the dc/dc buck converter will work with smaller duty cycle, producing more losses in switching due to high f_s, the efficiency of the converter will reduce.

2) Capacitor Design: In the unity PFC operation, as the input voltage and current are in the same phase, the oscillations in the input power are double the frequency of the line. Because of the constant load (dc power output), the voltage across the capacitor terminal at the dc bus (V_{BUS}) rises by storing the surplus energy when the load demand is less than the supplied power. Similarly, it releases its stored energy to discharge in the load as counter phenomena. Subsequently, V_{BUS} likewise oscillates at the second harmonic frequency of the fundamental

$$\text{i.e. } V_{\mathrm{BUS,AC}} \approx \frac{P_m}{2\omega C_1 V_{\mathrm{BUS}}}\sin\left(2\omega t\right). \qquad (17)$$

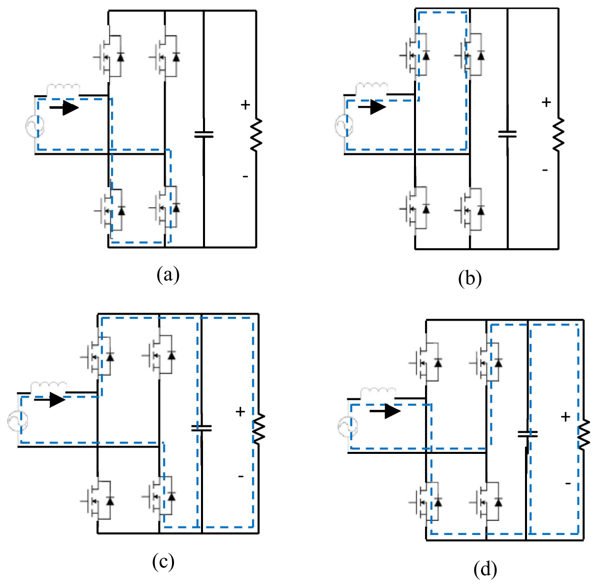

Fig. 10. Operation modes of the PWM boost rectifier.

The second ripple in the capacitor at the dc bus fluctuates with a frequency of switching set by the boost switch modulation. In this case, the magnitude of the ripple is lesser than that in the first one, yet its frequency is much higher

$$\Delta V_{\mathrm{BUS}} = \frac{I_{L_{\mathrm{DC}}}\langle d_{\mathrm{DC}}\rangle\langle d_{\mathrm{AC}}\rangle}{f_s C_1}. \qquad (18)$$

The capacitor must be designed to tackle both the ripples.

B. Operation and Working of the PWM Boost Rectifier

Fig. 10 demonstrates the four working conditions of the PWM rectifier [26]. Now, for Modes I and II, the ac source is shorted if either pair of switches $S_2 - S_4$ or $S_1 - S_3$ is connected. In this situation, H-bridge voltage input (V_{br}) is zero but the current through the inductor increases. For Mode III, switch pair $S_1 - S_4$ is connected and V_{br} equals V_{BUS}. In this operating mode, the load is associated with the input side. Mode IV is just like Mode III, anyway for this situation, switch pair $S_2 - S_3$ is connected and V_{br} equivalents to $-V_{\mathrm{BUS}}$ [see Fig. 10(b)].

Due to the unity power factor consideration, the input current and voltage are in the same phase. Subsequently, the input power and the output voltage of the PWM rectifier will oscillate twice comparing to line frequency as represented in Fig. 10(a).

Now the ripple in the output voltage of the PWM rectifier is so high that it cannot be applied directly to the EV battery, hence, the second stage of the dc/dc (buck/boost) converter is desirable for the EV charging circuit. The PWM boost rectifier simulation results are shown in Fig. 11.

VI. Simulation Results

The circuit schematics of the solar PV system of the PHEV charging analyzed in Fig. 8, it is obligatory for simulation studies to be performed in MATLAB (Simulink) software program. Hence, a correct realization of a solar off-grid PV-EV charging

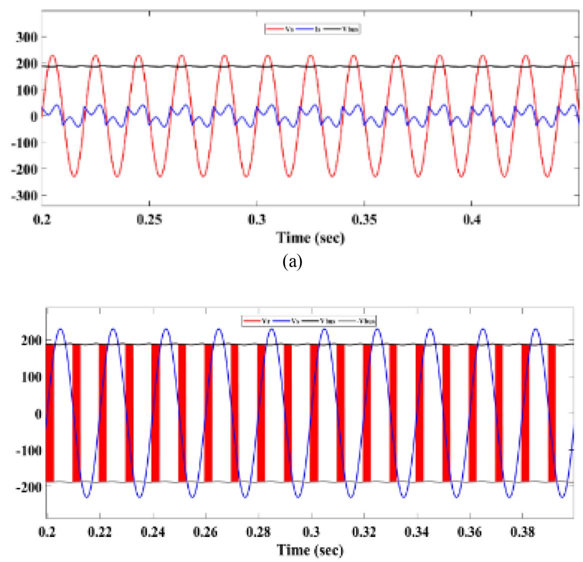

Fig. 11. PWM rectifier operation results are shown through simulation. (a) Input current, input voltage, and dc bus voltage waveforms. (b) H-bridge input voltage and input voltage.

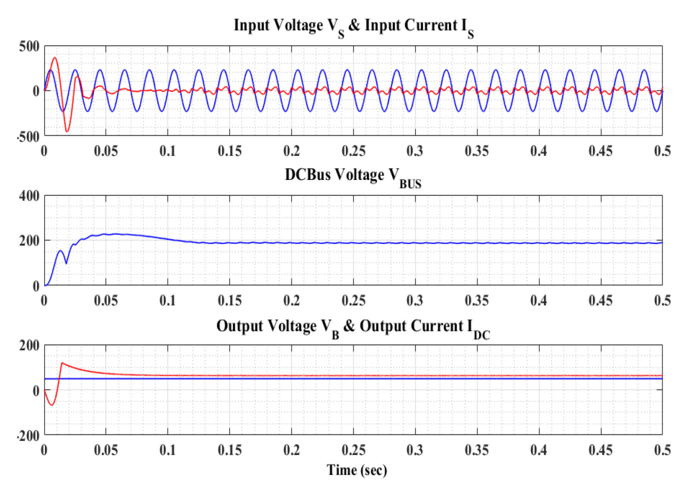

Fig. 12. Simulation results for a solar-powered EV battery charger circuit. (a) Input voltage and current graph. (b) DC bus voltage graph. (c) Output voltage and current graph.

station in the real estimate of time might be achievable. The performance of the EV charging system is limited by its output power rating, i.e., the capacity to transfer the energy to charge the EV battery pack on the specified rate determined by the battery C rating.

Fig. 12 presents the simulation results for a solar-powered EV battery charger circuit, viz., the input voltage and current waveform, the dc bus voltage waveform, and the output voltage and current waveform, respectively. In the proposed design of a solar PV system, inverter modeling is not carried out. Its function is to perform dc to ac conversion of dc generated output by solar panels. Generally, the inverters have higher efficiency, and hence, the PV system performance is not affected much. Here, the simulation result shown in the first graph (i.e., input voltage and current waveform) is the output of the inverter which is 50 Hz, 230 V_{AC}, and it is the input to the EV battery charger as well. Based on the information from simulation studies, a hardware implementation of a solar-based EV charging station cited at CARET, AMU, Aligarh region could be analyzed and developed.

TABLE III
SIMULATION RESULT INDICATED IN THE SIMULATION MODEL

LED position	Description
LED D5	Turns ON: Code for Arduino is debugging properly
LED D4	Turns ON: the Pilot pin is connected
LED D3	Turns ON: Car is requesting a charge
LED D2	Turns ON: Car is charging

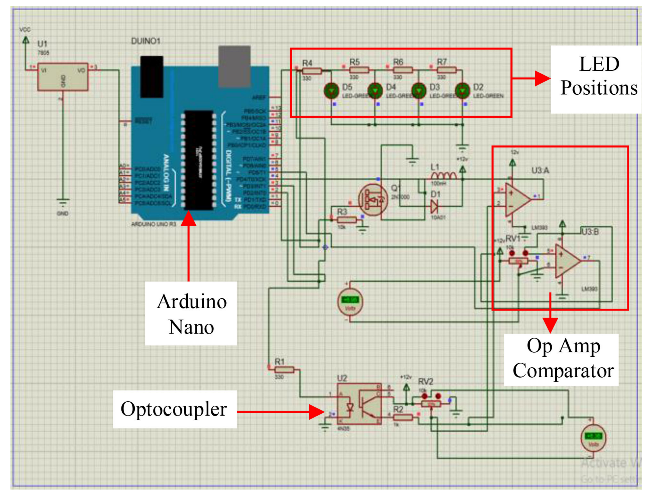

Fig. 13. Signaling circuit simulation in PROTEUS software displaying the LED condition.

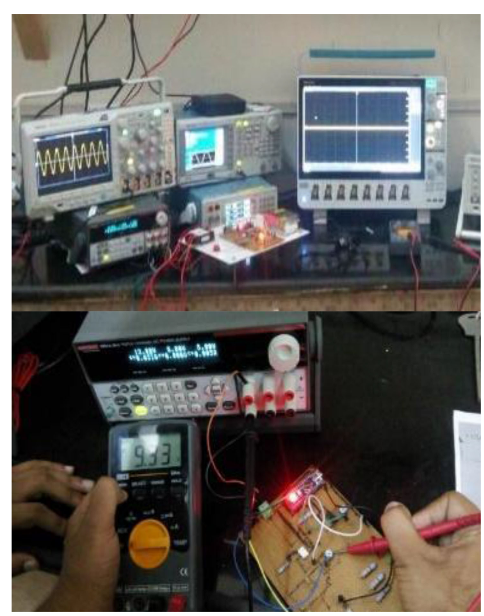

Fig. 14. Experimental setup and testing of a prototype hardware model in the EV hardware in loop (HIL) Lab, CARET at AMU.

This article has been accepted for inclusion in a future issue of this journal. Content is final as presented, with the exception of pagination.

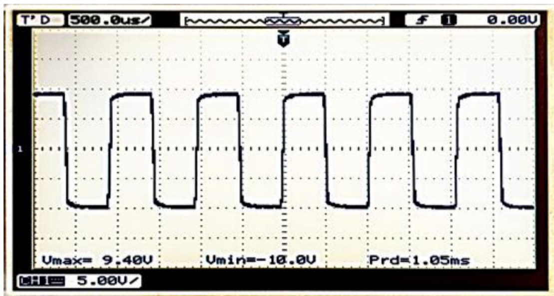

Fig. 15. Square PWM waveform of 1 kHz for state B.

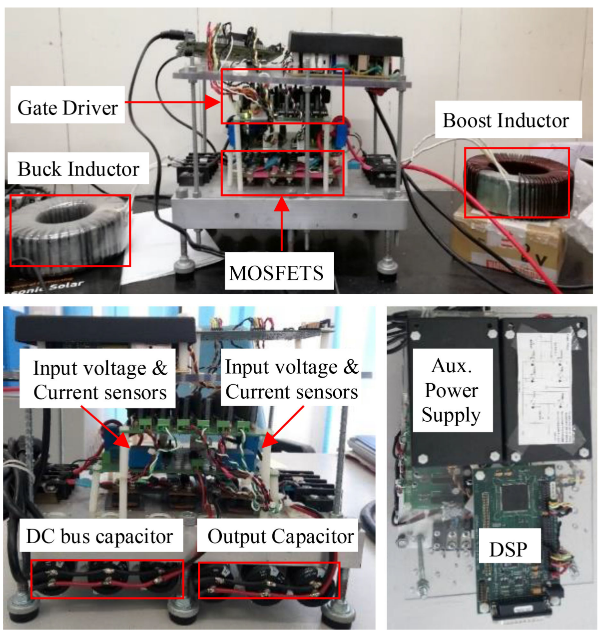

Fig. 16. Hardware setup and components of the battery charger circuit.

A. Modeling and Simulation of Controller Circuit

The communication and signaling circuit is simulated in PROTEUS software based on Arduino Nano, we can use any microcontroller for the PWM, the reason for using Arduino is that it is very versatile and easy to program.

When we give run command to the software, the circuit simulated based on Arduino coding accordingly as follows.

Table III depicts the sequence of states depending on the charging condition of Table II, and Fig. 13 shows only blinking LED state (i.e., charging state).

B. Lab Prototype Model

The prototype hardware setup in the lab is described here. The results obtained from PROTEUS simulation and a consecutive hardware implementation show that the proposed controller can detect all six states as required for proper operation of the charger.

The experimental setup is developed in the EV Hardware-In-the-Loop Lab (see Fig. 14) established at CARET in AMU campus. The model is tested in the lab and the multimeter gives

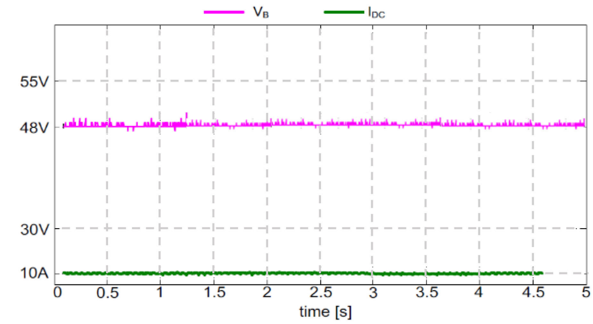

Fig. 17. Experimental waveforms representing the load variation response of a dc–dc converter (buck) in the charging mode.

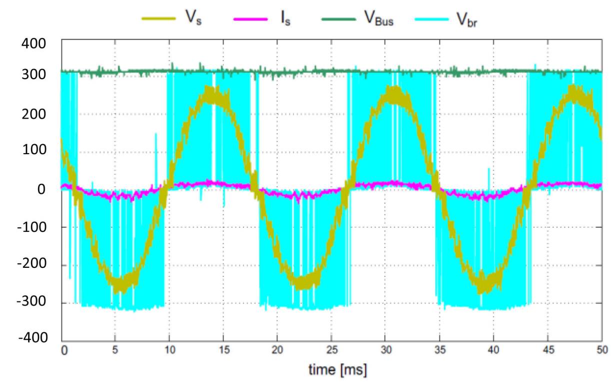

Fig. 18. Experimental waveforms of the PFC stage.

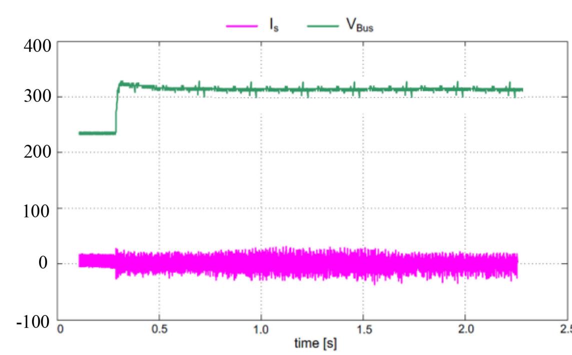

Fig. 19. Experimental waveforms representing the load variation response at the ac–dc converter stage.

9.33 V on the display. Fig. 15 shows a 1 kHz PWM square waveform for state B (+9 V) of the signaling circuit (at 40% duty cycle).

VII. Hardware in the Loop and Experimental Verification

Considering the design given in the earlier sections, the charger circuit used in the EV (see Fig. 8) could be realized practically as depicted in Fig. 16.

The sensor feedback input has been executed through the DSP TMS320F2812 board. The voltage and current sensors

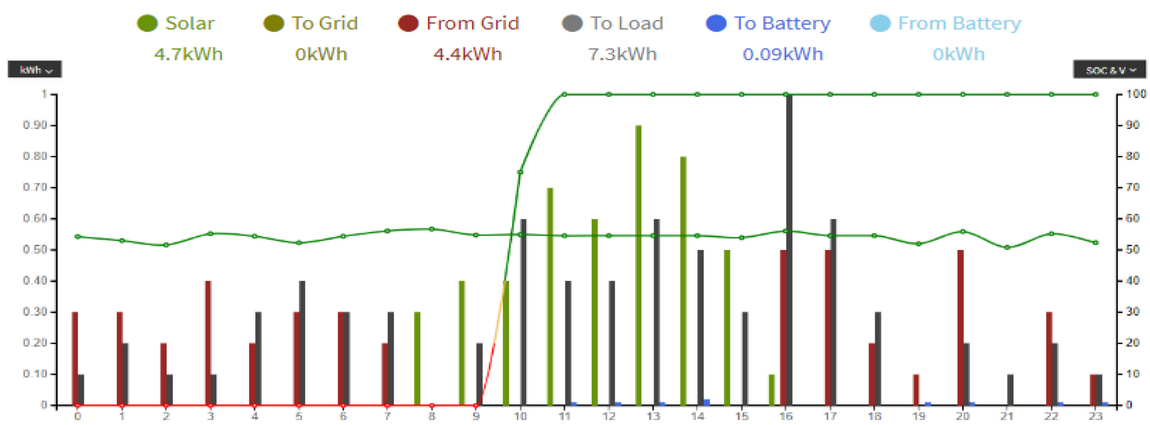

Fig. 20. Graphical representation of various charging parameters, viz. SOC, solar grid, etc.

are LV20-P 500V and LA100-P 100A, respectively. Microsemi MOSFET switch APT100M50J, 500 V, and 100 A rated are triggered through VLA513 at 60 kHz frequency, IGBT-Powerex drivers. An ac voltage regulated supply is supplying the voltage input to the electronic dc (output) load. The whole feedback controller has been executed digitally in the DSP.

The current and voltage output waveforms in this operation mode (charging) of the dc/dc second stage buck converter under dynamically changing load conditions is shown in Fig. 17. Here, in the charging mode, the second stage manages the dc inductor current $I_{\rm DC}$ constant through the current controller, when the load (resistive in this case) changes.

The second stage dc/dc bidirectional converter works in the buck operating mode to reduce the voltage at the dc bus $(V_{\rm BUS})$ to the level of the voltage of the battery terminal (V_B). In the ac/dc rectifier operation, the PWM converter in the boost mode maintains the PFC (in an active mode). The PWM pulses from the DSP board deals with the actuation of various switching appropriately in +ve and −ve half cycles of the voltage input. Fig. 18 demonstrates the experimental waveforms in a PWM boost PFC stage. Similarly, the results are shown in the simulation of Fig. 11, the controller keeps up the PFC and, therefore, the input voltage and current are in the same phase.

Moreover, as calculated by (17), the dc bus voltage fluctuates double the fundamental frequency. Here, the power factor is 0.93. The PFC corrected it from 0.72. Because of the ac power supply internal impedance, the switching phenomena are replicated in the input side voltage waveform. In addition, hence, a little increment in the THD value is caused.

Fig. 19 shows how the ac/dc rectification stage responds to the variation in the load. For this situation, a compensator (feedforward) is additionally executed in the controller algorithm. Because the PFC has average mode multiloop current control, the voltage at the dc bus $(V_{\rm BUS})$ is kept steady, yet the variation in the load must be seen by the variation in the magnitude of the input side current waveform.

The energy management controller is used for display and real-time monitoring of the plant, as shown in Fig. 1 via Ethernet cable as explained in Section II. In Fig. 20, different parameters of the SPVCS are shown graphically.

VIII. Conclusion

The electrified transportation, i.e., EV and PHEV offers a noise free, clean, and efficient means of transportation system as compared to the internal combustion engine vehicle (ICEV). Also, renewable energy (RE) sources (solar energy) are easily integrated with the refueling system of these vehicles. Therefore, the work presented in this article is an exhaustive study for designing, modeling, simulation, and hardware realization of an EV charging station with solar PV source. Various segments, for instance, recharging infrastructure, approach and methodology adopted, and communication, signaling, and control aspects applicable to the EV charging process through the EVSE has been discussed in detail. In this article, the PEV is furnished with a charging circuit of the battery, which must be able to maintain the power factor near unity (approx. 0.95) through PFC at the input terminal and a low current ripple through the filter circuit at the output terminal. For this reason, a PWM boost rectifier used as in cascade connection with a dc/dc buck converter has been suggested in this article. The circuit operation has been examined through mathematical modeling for the charging condition in the CCM mode has been done. A DSP controller board for the proper operation of the circuit with respect to the steady-state operation of the PFC, the transient response of the circuit as well as the dynamic EV charging load response based on the SOC, has also been shown. Moreover, the inference from the simulation results shows that the performance of the overall system depends on solar radiation and the battery SOC. Compared with the empirical methods of calculation/sizing with assumed data, as illustrated by the literature survey (see Section I) for an off-grid PV system, the direct and applied approach with designed data, the MATLAB-based Simulink model will provide the simulation, sizing, and implementation for a complete PV-EV charging system in a comparatively shorter time. Hence, the results are consistent with both the literature part and the present state of the proposed solar-based EV charging framework at CARET building parking area.

Challenges and Future Work

The solar-powered EV charging stations have barriers for deployment at a large scale. For a PV system, the intermittency and only daytime generation restrict its use from meeting a big fraction of electricity consumption. Obviously, numerous technological advancements are on the prospect to be recognized for the future production of automobiles, the key challenges still need to be notified in the field of cost, weight, and volume to meet the required performance criteria. Additionally, some more issues are related to manufacturability, safety, robustness, consistency, etc. Significant challenges include the following.

1) The economic and performance criteria for the battery as a storage element that limits their profitable consumption. In addition, also has a limited utility as well as owing to driver range anxiety and charging infrastructure access. Accordingly, the EV charging infrastructure and their opportunity options should be considered by deploying a particular charging infrastructure with the selected business opportunity seems to overcome the range anxiety impact and increase utility.
2) Development of power electronic components for direct dc interconnection of the solar PV and EV systems. Barriers and challenges regarding direct dc PV charging of the EVs are lack of equipment and application standards for dc distribution, security, power protection device application, etc. Also, the robust ecosystem is not yet developed so far to sustain the use of dc in commercial level electrification.

In spite of the above mentioned challenges and roadblocks, if both the technologies integrated to deploy simultaneously, the improved, efficient, and economic operation might be feasible of the EV and its daytime charging by means of free electricity, and hence, extending the range while decreasing the battery storage needed. The best optimally feasible alternative is to install the solar charging infrastructure at different locations globally. Speeding up the placement of the renewable energy-based generation and the EVs in the transportation sector would enhance economic development.

References

[1] S. M. Amrr, M. S. Alam, M. S. J. Asghar, and F. Ahmad, "Low cost residential microgrid system-based home to grid (H2G) back up power management," *Sustain. Cities Soc.*, vol. 36, pp. 204–214, 2018.

[2] N. Saxena, I. Hussain, B. Singh, and A. L. Vyas, "Implementation of a grid-integrated PV-battery system for residential and electrical vehicle applications," *IEEE Trans. Ind. Electron.*, vol. 65, no. 8, pp. 6592–6601, Aug. 2018.

[3] S. Khan, A. Ahmad, F. Ahmad, M. Shafaati Shemami, M. Saad Alam, and S. Khateeb, "A comprehensive review on solar powered electric vehicle charging system," *Smart Sci.*, vol. 6, no. 1, pp. 54–79, Jan. 2018.

[4] M. Shafaati Shemami, M. Saad Alam, and M. S. J. Asghar, "Fuzzy control assisted vehicle-to-home (V2H) energy management system," *Smart Sci.*, vol. 6, no. 2, pp. 173–187, Apr. 2018.

[5] F. Luo, G. Ranzi, W. Kong, Z. Y. Dong, and F. Wang, "Coordinated residential energy resource scheduling with vehicle-to-home and high photovoltaic penetrations," *IET Renewable Power Gener.*, vol. 12, no. 6, pp. 625–632, 2018.

[6] S. Sahoo, S. Prakash, and S. Mishra, "Handshaking V2G strategy for grid connected PV assisted charging station," *IET Renewable Power Gener.*, vol. 11, no. 11, pp. 1410–1417, 2017.

[7] F. Ahmad, M. S. Alam, and S. M. Shariff, "A cost-efficient energy management system for battery swapping station," *IEEE Syst. J.*, to be published, doi: 10.1109/JSYST.2018.2890569.

[8] J. Cao, C. Crozier, M. Mcculloch, and Z. Fan, "Optimal design and operation of a low carbon community based multi-energy systems considering EV integration," *IEEE Trans. Sustain. Energy*, vol. 10, no. 3, pp. 1217–1226, Jul. 2019.

[9] T. Konjedic, "Control of integrated single-phase PFC charger for EVs," *IET Power Electron.*, vol. 11, no. 11, pp. 1804–1812, 2018.

[10] S. A. Khan, Y. Guo, R. Islam, and J. Zhu, "A new isolated multi-port converter with multi-directional power flow capabilities for smart electric vehicle charging stations," *IEEE Trans. Appl. Supercond.*, vol. 29, no. 2, pp. 1–4, Mar. 2019.

[11] S. A. Singh, G. Carli, S. S. Williamson, and N. A. Azeez, "Modeling, design, control, and implementation of a modified Z-source integrated PV/grid/EV DC charger/inverter," *IEEE Trans. Ind. Electron.*, vol. 65, no. 6, pp. 5213–5220, Jun. 2018.

[12] K. M. Muttaqi, R. Islam, and D. Sutanto, "Future power distribution grids: Integration of renewable energy, energy storage, electric vehicles, superconductor, and magnetic bus," *IEEE Trans. Appl. Supercond.*, vol. 29, no. 2, pp. 1–5, Mar. 2019.

[13] V. Monteiro, J. C. Ferreira, A. A. Melendez, C. Couto, and J. L. Afonso, "Experimental validation of a novel architecture based on a dual-stage converter for off-board fast battery chargers of electric vehicles," *IEEE Trans. Veh. Technol.*, vol. 67, no. 2, pp. 1000–1011, Feb. 2018.

[14] G. R. C. Mouli, J. Schijffelen, M. van den Heuvel, M. Kardolus, and P. Bauer, "A 10 kW solar-powered bidirectional EV charger compatible with Chademo and COMBO," *IEEE Trans. Power Electron.*, vol. 34, no. 2, pp. 1082–1098, Feb. 2019.

[15] C. Shi, Y. Tang, and A. Khaligh, "A three-phase integrated onboard charger for plug-in electric vehicles," *IEEE Trans. Power Electron.*, vol. 33, no. 6, pp. 4716–4725, Jun. 2018.

[16] P. Shrivastava, M. S. Alam, and M. S. J. Asghar, "Design and techno-economic analysis of plug-in electric vehicle-integrated solar PV charging system for India," *IET Smart Grid*, vol. 2, no. 2, pp. 224–232, Jun. 2019.

[17] F. Ahmad, M. S. Alam, and M. Asaad, "Developments in xEVs charging infrastructure and energy management system for smart microgrids including xEVs," *Sustain. Cities Soc.*, vol. 35, pp. 552–564, 2017.

[18] A. Khaligh and M. D. Antonio, "Global trends in high-power on-board chargers for electric vehicles," *IEEE Trans. Veh. Technol.*, vol. 68, no. 4, pp. 3306–3324, Apr. 2019.

[19] A. Ahmad, M. S. Alam, and R. Chabaan, "A comprehensive review of wireless charging technologies for electric vehicles," *IEEE Trans. Transport. Electrific.*, vol. 4, no. 1, pp. 38–63, Mar. 2018.

[20] S. Khan, S. Shariff, A. Ahmad, and M. S. Alam, "A comprehensive review on level 2 charging system for electric vehicles," *Smart Sci.*, vol. 477, pp. 1–23, Jul. 2018.

[21] M. S. Alam *et al.*, "A bibliographical review of electrical vehicles (xEVs) standards," *SAE Int. J. Alternative Powertrains*, vol. 7, no. 1, pp. 63–98, Apr. 2018.

[22] F. Ahmad and M. S. Alam, "Economic and ecological aspects for microgrids deployment in India," *Sustain. Cities Soc.*, vol. 37, pp. 407–419, Feb. 2018.

[23] M. S. Alam, M. F. Azeem, and A. T. Alouani, "Modified queen-bee algorithm-based fuzzy logic control for real-time robust load matching for a solar PV system," *IEEE Trans. Sustain. Energy*, vol. 5, no. 2, pp. 691–698, Apr. 2014.

[24] G. S. Misyris, D. I. Doukas, T. A. Papadopoulos, D. P. Labridis, and V. G. Agelidis, "State-of-charge estimation for Li-ion batteries: A more accurate hybrid approach," *IEEE Trans. Energy Convers.*, vol. 34, no. 1, pp. 109–119, Mar. 2019.

[25] M. Restrepo, J. Morris, M. Kazerani, and C. A. Cañizares, "Modeling and testing of a bidirectional smart charger for distribution system EV integration," *IEEE Trans. Smart Grid*, vol. 9, no. 1, pp. 152–162, Jan. 2018.

[26] F. J. B. Brito, Jr., S. Daher, P. T. Bascop, B. B. Chaves, D. P. Damasceno, and B. R. de Almeida, "Design and control for a single-phase/-stage buck/boost-type PWM PFC rectifier," in *Proc. IEEE Int. Conf. Ind. Appl.*, 2018, pp. 530–536.

Samir M. Shariff (SM'00) received the B.S. and M.S. degrees in electrical and computer engineering from Washington University, St. Louis, MO, USA, in 1994 and 1996, respectively, and the Ph.D. degree in electrical and computer engineering from Wichita State University, Wichita, KS, USA, in 2009.

He is currently an Associate Professor with the Department of Electrical Engineering, College of Engineering, Taibah University, Medina, Saudi Arabia, where he is also leading the industrial collaborative interdisciplinary research in electrical engineering, and is also the Head of the Strategic Research Unit. His research interests include smart microgrids, electric vehicles, renewable energy technologies, and power electronics.

Mohammad Saad Alam (S'02–M'10–SM'16) received the B.Tech. degree in electrical engineering from Aligarh Muslim University (AMU), Aligarh, India, in 2003, the M.S. degree in electrical and computer engineering from the Illinois Institute of Technology, Chicago, IL, USA, in 2005, and the Ph.D. degree in electrical engineering from Tennessee Tech University, Cookeville, TN, USA, in 2009.

He is currently an Associate Professor of electrical engineering with AMU, and the Coordinator of the Center of Advanced Research in Electrified Transportation, AMU, Aligarh, India.

Dr. Alam is a member of the Inter-Ministry Technology Advisory Group with the Department of Heavy Industry to support the FAME mission of the Government of India, at the national level. At the international level, he is a member of the SAE Task Force, where he is involved in developing the international standards for the interoperability of EVs and PHEVs with the smart grids. He is an Associate Editor for the IEEE TRANSACTIONS ON TRANSPORTATION ELECTRIFICATION and Springer *Journal of Modern Power System and Clean Energy*.

Furkan Ahmad (S'17) received the B.Tech. degree in electrical engineering and the M.Tech. degree in electrical engineering with specialization in high voltage and insulation engineering, in 2012 and 2015, respectively, from Aligarh Muslim University, Aligarh, India, where he is currently working toward the Ph.D. degree in power system and drives.

Since January 2018, he has been a CSIR-Senior Research Fellow. His research interests include smart microgrids, electric vehicles, energy management, power market operations, and renewable energy integration.

Mr. Ahmad was the recipient of the 2016–2017 CSIR Junior Research Fellowship Award.

Yasser Rafat received the B.Tech. degree in mechanical engineering from Aligarh Muslim University (AMU), Aligarh, India, in 2003, the master's degree from Concordia University, Montreal, QC, Canada, in 2007, and the Ph.D. degree from McGill University, Montreal, QC, Canada, in 2013.

He is currently an Assistant Professor with the Department of Mechanical Engineering, AMU, and is the Assistant Training and Placement Officer. He is the Lab Incharge of the Turbomachinery Lab. He is among the founding members of an industrial collaborative research center in electric mobility at AMU and is the Co-Coordinator of the Center of Advanced Research in Electrified Transportation. He has authored or coauthored several publications and delivered talks in the area of thermofluids and thermoacoustics. His research interests include the fields of sports projectile aerodynamics, quantification of Schlieren visualization data of turbulent jets, heat management of Li-ion batteries, building acoustics, and thermoacoustic refrigerators and engines.

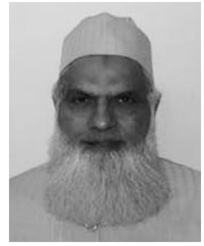

M. Syed Jamil Asghar (SM'94) received the B.Sc. Eng. degree in electrical engineering, the M.Sc. Eng. degree in power systems, and the Ph.D. degree in power electronics from Aligarh Muslim University (AMU), Aligarh, India, in 1978, 1982, and 1995, respectively.

He is currently a Professor with the Department of Electrical Engineering, AMU. He has established the Centre of Renewable Energy, Department of Electrical Engineering, funded by Government of India. He is the Coordinator of DRS program under Special Assistance Program of University Grants Commission, Government of India. He has successfully completed many Government funded research projects. He has several patents to his credit related to renewable energy (total 18 patents). He has authored or coauthored more than 60 papers in refereed journals and conference proceedings including several single-authored papers in the IEEE transactions (USA). His research interests include power electronics, renewable energy systems, and electrical machines.

Dr. Asghar is a Fellow of the Institution of Electronics and Telecommunication Engineers (India).

Saadullah Khan received the B.E. degree in electrical engineering and the M.Tech. degree in electrical engineering (instrumentation and control) from Aligarh Muslim University, Aligarh, India, in 2013 and 2018, respectively.

His research interests include electric vehicles, charging infrastructure, renewable energy integration, etc.